

Supporting Information

Integrating 3D Printing and Self-Assembly for Layered Polymer/Nanoparticle Microstructures as High-Performance Sensors

Sayli Jambhulkar^a, Weiheng Xu^a, Rahul Franklin^b, Dhraheedhar Ravichadran^a, Yuxiang Zhu^a, Kenan Song^{*c}

^a *Systems Engineering, The Polytechnic School of Engineering (TPS), Ira A. Fulton School of Engineering, Arizona State University, Mesa, AZ, USA 85281*

^b *Materials Science and Engineering, The School for Engineering of Matter, Transport and Energy (SEMTE), Ira A. Fulton School of Engineering, Arizona State University, Mesa, AZ, USA 85287*

^c *The Polytechnic School of Engineering (TPS), The School for Engineering of Matter, Transport and Energy (SEMTE), Ira A. Fulton School of Engineering, Arizona State University, Mesa, AZ, USA 85281.*

Experimental Section

Preparation of aligned CNF on 3D printed pattern:

The epoxy substrate, having triangular gratings, was printed by stereolithography printing SLA (Formlabs 2 stereolithographic printer from Formlabs) through layer-by-layer curing of a photosensitive resin, a mixture of the methyl acrylate oligomer/monomer, and the photoinitiator ordered from Formlabs, which was used as obtained. The design consisted of a triangular grating of an approximate height of 75 μm , a base of 100 μm , and spacing between the channels of 200 μm over a 1 \times 1 cm^2 sample area. After printing, patterns were thoroughly cleaned in isopropyl alcohol (IPA, $\geq 99.7\%$, FCC, FG, Sigma-Aldrich) and cured at 55 $^\circ\text{C}$ for 40 minutes in a Form UV curing chamber to achieve a robust substrate. The suspension of THF and CNF was obtained by the addition of 1, 5, 10, and 100 mg of CNF (length 20 - 200 μm and a diameter of 100 nm, Sigma-Aldrich) into 10 ml of tetrahydrofuran (THF, anhydrous, $\geq 99.9\%$, inhibitor-free, Sigma-Aldrich) to make 0.1, 0.5, 1, and 10 $\text{mg}\cdot\text{ml}^{-1}$ dispersion. Later, the dispersion was mixed by a vortex mixer for 5 minutes and was sonicated for 24 hr. The 3D printed polymer patterns were immersed into well-dispersed CNF/THF suspensions with desired orientation in vacuum at 50 $^\circ\text{C}$.

Fabrication of CNF-epoxy electrodes, and electrical/sensing measurements:

The *CNF-epoxy* electrode was prepared by attaching conductive aluminum wires at the ends of CNF coated samples surfaces via silver paste adhesive. The contacts were maintained at a distance of 8mm from each other and coated with a quick setting epoxy 9160 to avoid interaction of the VOC with the silver paste. The electrical conductivity of CNF was studied using a PARSTAT-2273 potentiostat from Princeton Applied Research. The I-V data were recorded from -2 to 2 V at an interval of 0.1 V. The sensitivity of the fabricated devices to VOCs was measured by a Keithley DMM7510 7 1/2 digital multimeter. All sensing responses were analyzed by measuring the resistance change across the two contacts when exposed to analytes. The chemical sensing measurements were taken using both the vapor and the droplet methods. In the gas method, a self-made test chamber was connected to a digital multimeter to record electrical resistance (Figure S4). The bubbler was filled with approximately 15 ml of VOC bath and dry air was passed through it with a controlled flow rate 10, 30, 50, 80, and 100 ml/min. Then, VOC vapors, along with dry air of different flow rates maintained with a total flow rate of 200ml/min, were passed to the CNF-epoxy electrode. The concentration of vapors in ppm (weight to the volume concentration of the VOCs) was calibrated by calculating the weight loss of the VOCs at different bubbling rates for 30 minutes at room temperature (RT). For sensing measurements at a different temperature, the methanol bath was heated by placing the bubbler on a hot plate and bubbled at a constant flow rate (160 $\text{ml}\cdot\text{min}^{-1}$). For recovery of initial resistance, the sample was exposed to air gas at 100 $\text{ml}\cdot\text{min}^{-1}$ for desorption of gas analytes. In the droplet method, 10 μL of each solvent was dropped over the substrate, and the resistance response was measured after the sample was immersed in the solvent. This method was repeated 5 times at 10-minute intervals for complete evaporation of the solvent.

Evaluation of laced liquor and human breath:

For breath sampling, volunteers consumed 150ml of an alcoholic beverage (Bacardi Limon Rum, 30% alcohol), and after every half hour, a BAC reading was taken with a Rofeer Alcohol Breathalyzer. Volunteers exhaled breath onto the sensor surface through a Teflon tube for 10 sec and the response was measured. For methanol sensing in laced alcoholic beverages, liquid samples were prepared by mixing 10 ml of Rum with 0, 0.5, 5, and 10 vol% of methanol. The samples were vigorously shaken for 30 sec to obtain uniform concentration. The liquid sample was placed in bubbles and air was blown at a fixed flow rate of 40 $\text{ml}\cdot\text{min}^{-1}$ the sensor was exposed to gases for 30sec, and readings were measured.

Surface characterization:

A 3D printed epoxy substrate was analyzed using true-surface microscopy (Witech alpha 300-RA) to check dimensions of surface patterning features. CNF and CNF-deposited samples were analyzed under a scanning electron microscope (SEM) at an accelerated voltage of 10kV. Samples were coated with Au-Pd for 80 sec to improve conductivity. Raman analysis of CNF samples was measured by Witech alpha 300RA+ with 532nm, 55 mW Nd: YAG laser line.

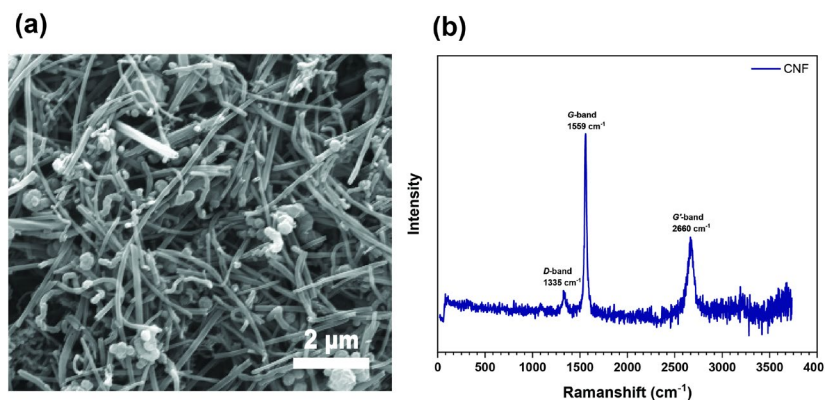


Fig. S1: (a) SEM image of CNF and (b) Raman spectra showing the D, G, and G' bands.

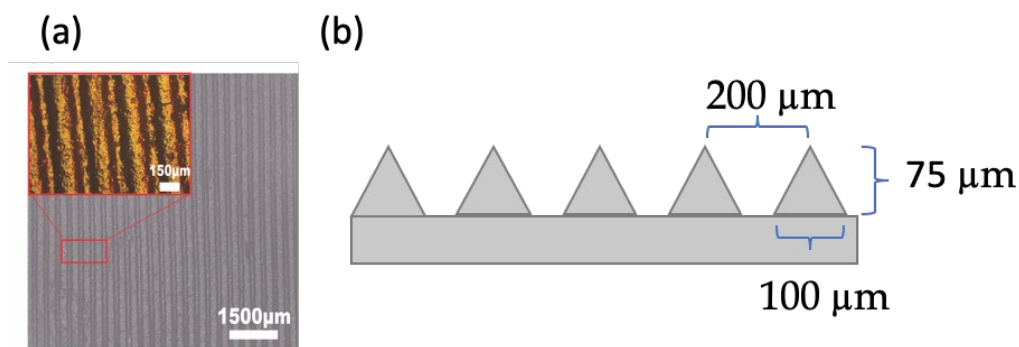


Fig. S2: (a) True surface micrograph of an epoxy substrate (top view) and (b) Schematic illustration of substrate dimensions (side view).

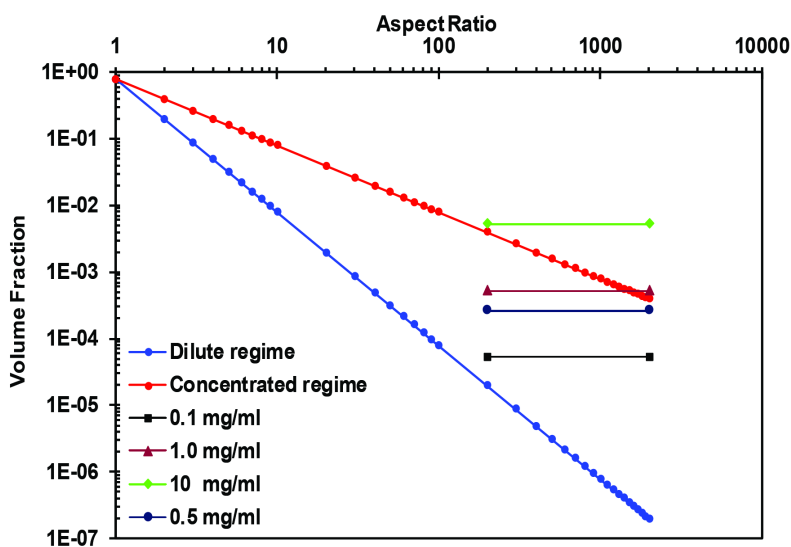


Fig. S3: CNF aspect ratio and volume fraction-based regimes (0.1,0.5mg/ml lie near semi dilute; 1mg/ml is in between semi dilute and concentrated; 10mg/ml is near concentrated).

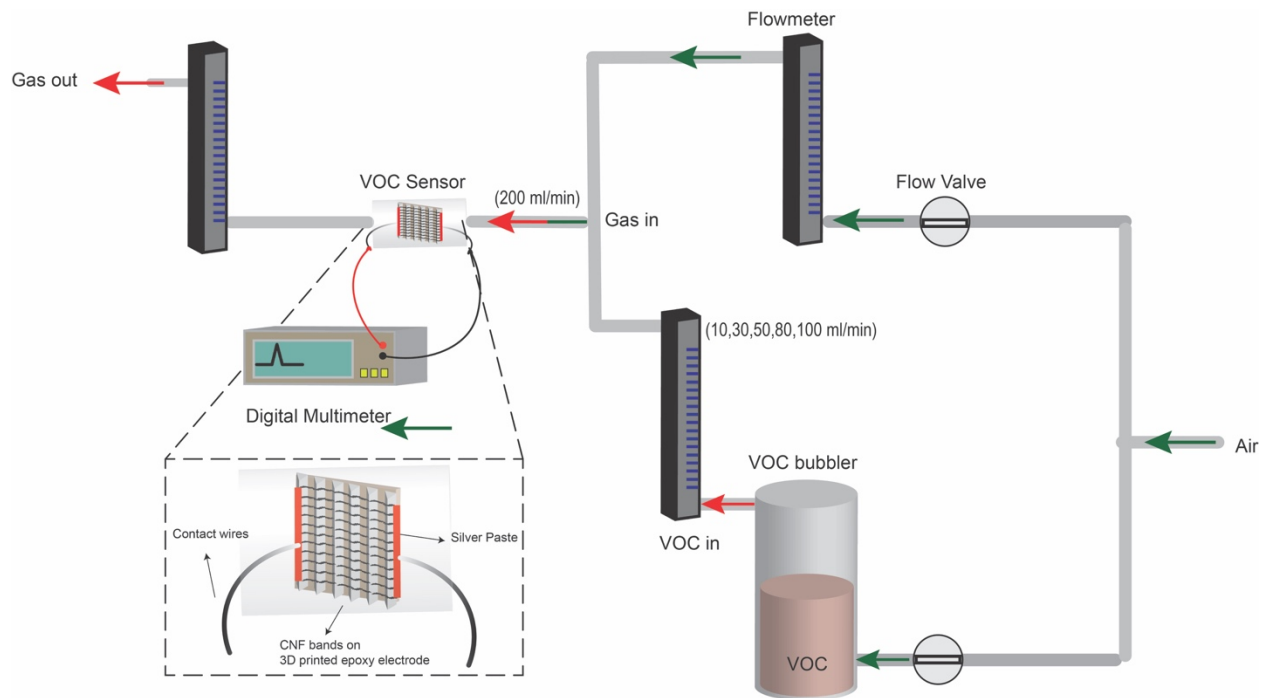


Fig. S4: In-house designed VOC gas sensing setup.

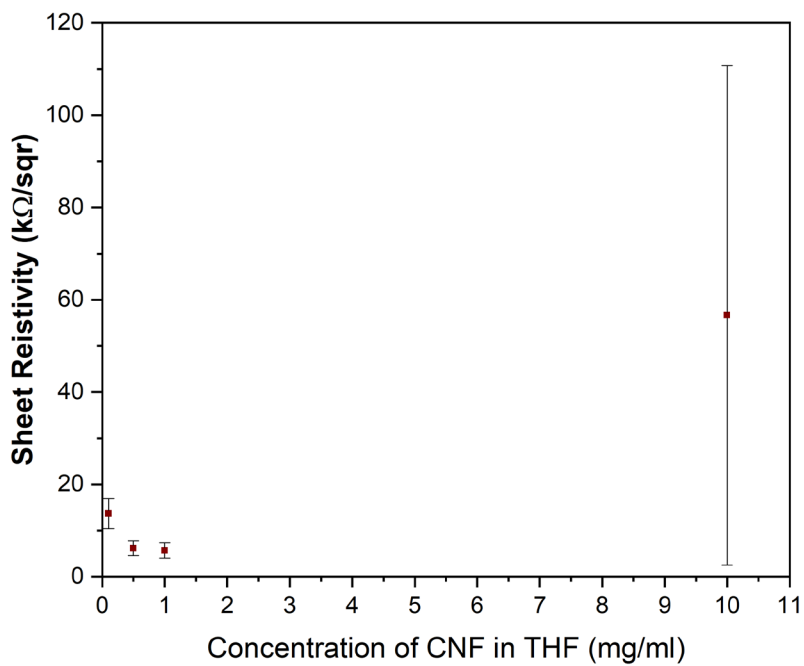


Fig. S5: The sheet resistivity of CNF coated substrate having different concentrations

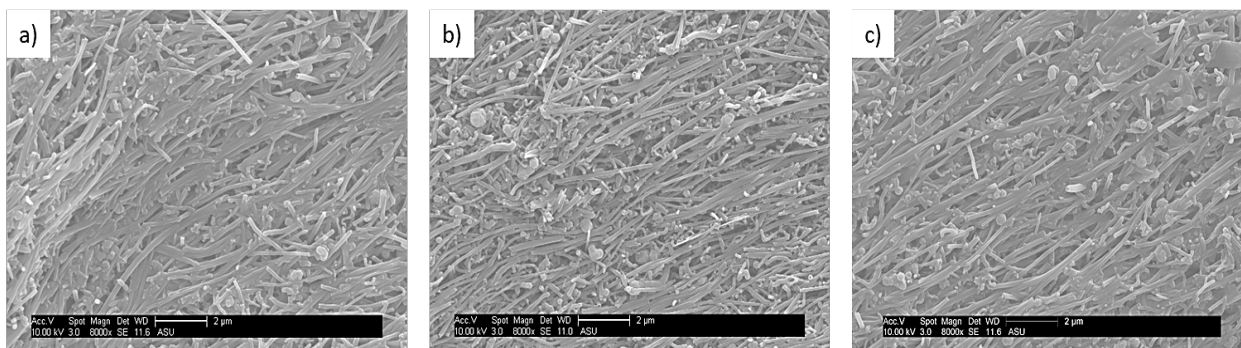


Fig. S6: SEM images at lower magnification showing an increase in CNF close packing with the concentration of nanoparticles a) E/CNF_{0.1}, b) E/CNF_{1.0}, and c) E/CNF_{10.0}.

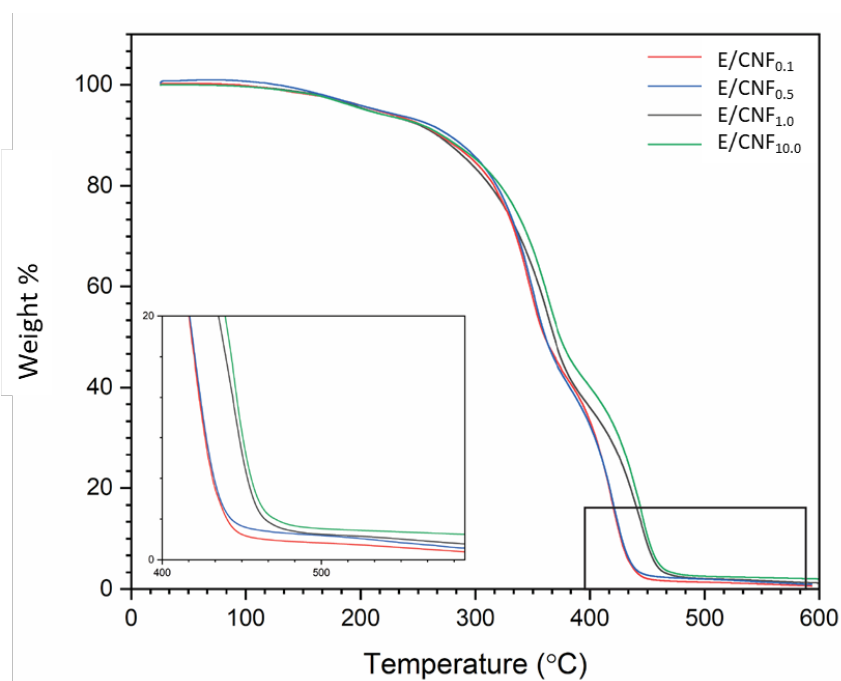


Fig. S7: TGA curve for different concentrations of CNFs

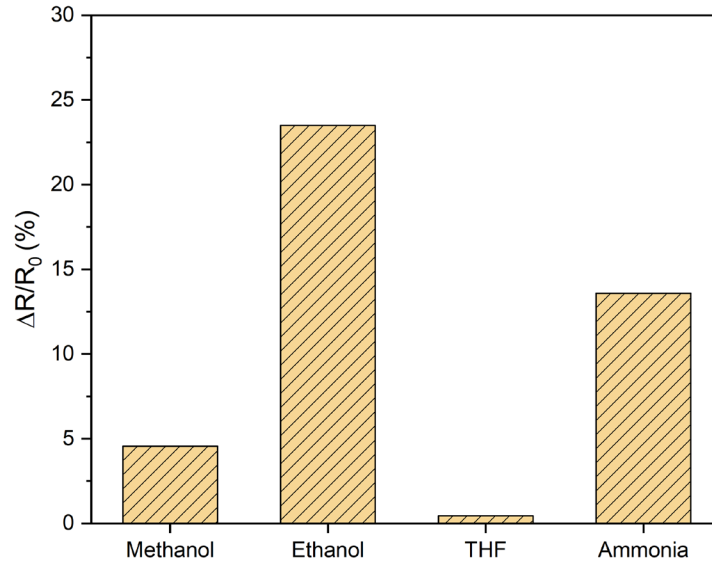


Fig. S8: Average gas response of E/CNF_{1.0} sensor to 100 ppm of various VOCs.

Table S1: Properties for the different analytes studied.

Solvent	Vapor pressure, kPa	Surface tension @25 °C (mN/m)	Dielectric constant (k)	Dipole moment (Debye)	Electric conductivity (μS/m)
DCM	58.2 ¹	28.1 ²	8.9 ³	1.60 ¹	4.30E-05 ²
Acetone	30.8 ⁴	23.3 ²	20.7 ⁵	2.88 ⁵	0.20 ²
Methanol	16.9 ¹	22.51 ⁶	32.6 ⁷	1.66 ⁷	3.8 ⁸
THF	21.6 ⁴	28 ²	7.52 ³	1.63 ¹	4.5E+01 ²
Ethanol	5.7 ⁴	21.82 ⁶	24.55 ⁵	1.69 ⁵	0.553 ⁹
Ammonia	74.46 ¹⁰	18.1 ¹¹	16.9 ¹¹	1.47 ¹²	5E+04 ¹³

Table S2: Previously reported gas reponse of 1D nanoparticles for 100 ppm of ethanol.

S.No.	Material	Temp(°C)	Response (S)	Ref.
1	Co ₃ O ₄ Micro rods	220	9.8 ^b	14
2	In ₂ O ₃ Microrods	300	18.33 ^a	15
3	LaFeO ₃ nanotubes	160	9.4 ^b	16
4	LaMnO ₃ /SnO ₂ nanofibers	260	20 ^a	17
5	SnO ₂ /ZnO Nanowires	400	14.1 ^a	18
6	SnO ₂ /Alpha Fe ₂ O ₃	350	6.2 ^a	19
7	Cu doped SnO ₂	300	13 ^a	20
8	CNT	RT	1.748 % ^c	21
9	CNT-Ti hybrid	RT	18.78 % ^c	21
10	CNT-Pt hybrid	RT	15.25 % ^c	21
11	CNT-Pd hybrid	RT	17.44 % ^c	21
12	CNT-ZnO	RT	1.06 ^a	22
13	RGO-SnO ₂	300	70 ^a	23
14	Exfoliated graphene	350	11 ^a	24
15	RGO/MoO ₃	110 RT	2.5 ^a 1.01 ^a	25
16	SnO ₂ -RGO	RT	3 ^a	26
17	Graphene-ZnO	300	210 ^a	27
18	CNT-ZnO	RT	6.1 ^a	22
19	This work	RT	23.5 %^c 1.25^a	-

$$^a S = R_a/R_g; ^b S = R_g/R_a; ^c S = (\Delta R/R_a) * 100\%;$$

Table S3: Previously reported Signal-to-Noise ratio of metal carbide for ethanol sensing

S. No.	Nanoparticles	Concentration (ppm)	SNR	Ref.
1	Alpha molybdenum carbide flakes	1000	600	28
2	Beta molybdenum carbide flakes	1000	333	28
3	Titanium carbide flakes	100	351	29
4	This work	100	553	-

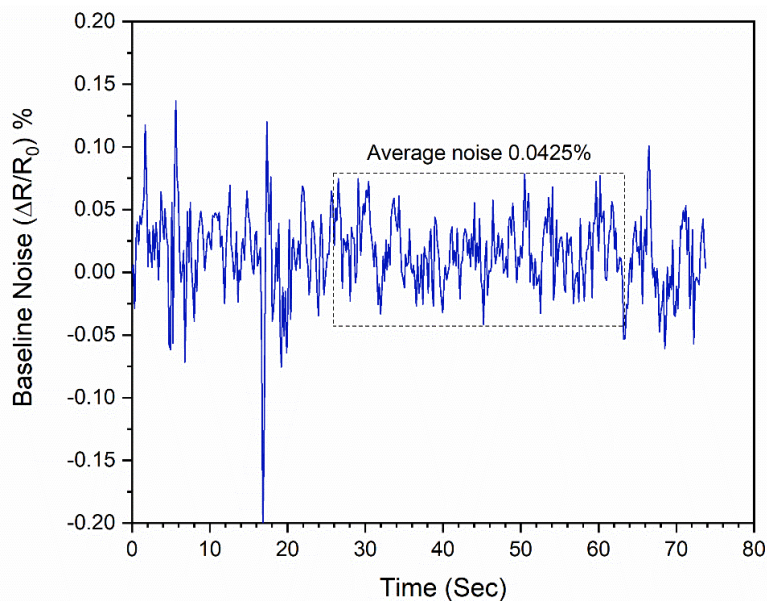


Fig. S9: Baseline noise of E/CNF_{1.0} sensor without any exposure to gas at RT.

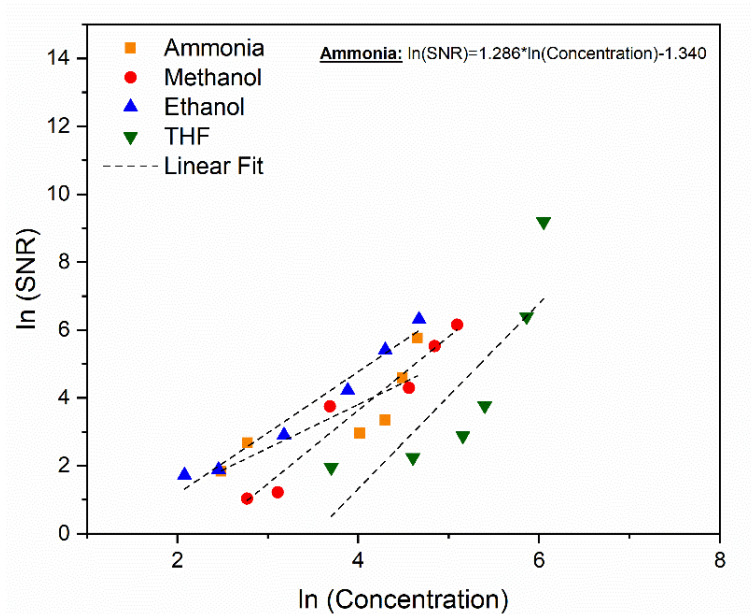


Fig. S10: Log-log plot of SNR vs. concentration for E/CNF_{1.0} sensor upon exposure to different concentrations of ethanol, methanol, THF, and ammonia. (dashed line and equation are derived by the fitting of the curve by power-law dependence)

Table S4: Previously reported limit of detection of metallic oxide nanoparticles for ethanol sensing

S. No.	Metal oxides	Limit of detection (ppm)	Ref.
1	ZnO/GO	10	27
2	Fe ₂ O ₃ nanofibers	100	19
3	Ag/TiO ₂ Nano belts	300	30
4	TiO ₂ /GO	100	31
5	PbS QDs, ZnO NRs	100	32
6	ZnO/MoS ₂	50	33
7	Co ₃ O ₄ -HHMS	100	34
8	This work	7.07	-

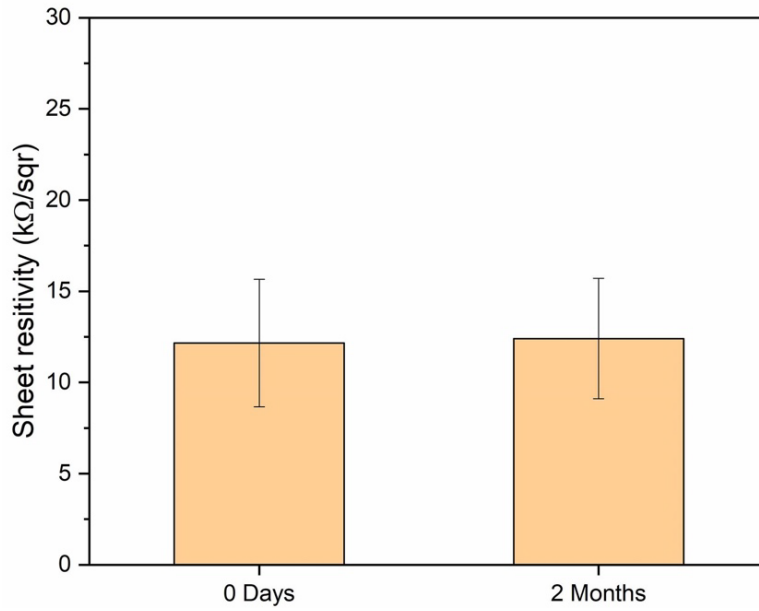


Fig. S11: Sheet resistivity of E/CNF_{1.0} sensor showing long term stability of sensor at ambient conditions.

References:

- 1 N. Lala, V. Thavasi and S. Ramakrishna, *Sensors*, 2009, **9**, 86–101.
- 2 *Poly Lactic Acid*, 2017, 10.
- 3 W. Pu, D. Fu, H. Xia and Z. Wang, *RSC Adv.*, 2017, **7**, 49828–49837.
- 4 M. Borelli, G. lasilli, P. Minei and A. Pucci, *Molecules*, 2017, **22**, 1306.
- 5 P. Di and D. P. Y. Chang, 13.
- 6 G. Vazquez, E. Alvarez and J. M. Navaza, *J. Chem. Eng. Data*, 1995, **40**, 611–614.
- 7 I. Hafaiedh, W. Elleuch, P. Clement, E. Llobet and A. Abdelghani, *Sensors and Actuators B: Chemical*, 2013, **182**, 344–350.
- 8 M. Farrokhi-Rad, *Ceramics International*, 2016, **42**, 3361–3371.
- 9 Y. R. Personna, L. Slater, D. Ntarlagiannis, D. Werkema and Z. Szabo, *Journal of Contaminant Hydrology*, 2013, **144**, 99–107.
- 10 T. A. Wilson, 60.
- 11 L. Haar and J. S. Gallagher, *Journal of Physical and Chemical Reference Data*, 1978, **7**, 635–792.
- 12 P. Pracna, V. Špirko and W. P. Kraemer, *Journal of Molecular Spectroscopy*, 1989, **136**, 317–332.
- 13 V. V. Shcherbakov, Yu. M. Artemkina, T. N. Ponomareva and A. D. Kirillov, *Russ. J. Inorg. Chem.*, 2009, **54**, 277–279.
- 14 W. Tan, J. Tan, L. Li, M. Dun and X. Huang, *Sensors and Actuators B: Chemical*, 2017, **249**, 66–75.
- 15 F. Huang, W. Yang, F. He and S. Liu, *Sensors and Actuators B: Chemical*, 2016, **235**, 86–93.
- 16 Y. Zhang, Z. Duan, H. Zou and M. Ma, *Materials Letters*, 2018, **215**, 58–61.
- 17 D. Chen and J. Yi, *J Nanopart Res*, 2018, **20**, 65.
- 18 D. T. Thanh Le, D. D. Trung, N. D. Chinh, B. T. Thanh Binh, H. S. Hong, N. Van Duy, N. D. Hoa and N. Van Hieu, *Current Applied Physics*, 2013, **13**, 1637–1642.
- 19 W. Zheng, Z. Li, H. Zhang, W. Wang, Y. Wang and C. Wang, *Materials Research Bulletin*, 2009, **44**, 1432–1436.
- 20 L. Liu, T. Zhang, L. Wang and S. Li, *Materials Letters*, 2009, **63**, 2041–2043.
- 21 S. Brahim, S. Colbern, R. Gump, A. Moser and L. Grigorian, *Nanotechnology*, 2009, **20**, 235502.
- 22 D. Zhang, Y. Sun and Y. Zhang, *J Mater Sci: Mater Electron*, 2015, **26**, 7445–7451.
- 23 W. Yuan and G. Shi, *J. Mater. Chem. A*, 2013, **1**, 10078.
- 24 M. Punginsang, A. Wisitsoraat, C. Sriprachuabwong, D. Phokharatkul, A. Tuantranont, S. Phanichphant and C. Liewhiran, *Applied Surface Science*, 2017, **425**, 351–366.
- 25 S. Bai, C. Chen, R. Luo, A. Chen and D. Li, *Sensors and Actuators B: Chemical*, 2015, **216**, 113–120.
- 26 C. A. Zito, T. M. Perfecto and D. P. Volanti, *Sensors and Actuators B: Chemical*, 2017, **244**, 466–474.
- 27 S. Liang, J. Zhu, J. Ding, H. Bi, P. Yao, Q. Han and X. Wang, *Applied Surface Science*, 2015, **357**, 1593–1600.
- 28 S.-Y. Cho, J. Y. Kim, O. Kwon, J. Kim and H.-T. Jung, *J. Mater. Chem. A*, 2018, **6**, 23408–23416.
- 29 S. J. Kim, H.-J. Koh, C. E. Ren, O. Kwon, K. Maleski, S.-Y. Cho, B. Anasori, C.-K. Kim, Y.-K. Choi, J. Kim, Y. Gogotsi and H.-T. Jung, *ACS Nano*, 2018, **12**, 986–993.
- 30 P. Hu, G. Du, W. Zhou, J. Cui, J. Lin, H. Liu, D. Liu, J. Wang and S. Chen, *ACS Appl. Mater. Interfaces*, 2010, **2**, 3263–3269.
- 31 E. Lee, D. Lee, J. Yoon, Y. Yin, Y. Lee, S. Uprety, Y. Yoon and D.-J. Kim, *Sensors*, 2018, **18**, 3334.
- 32 D. Zhang, G. Dong, Y. Cao and Y. Zhang, *Journal of Colloid and Interface Science*, 2018, **528**, 184–191.
- 33 H. Yan, P. Song, S. Zhang, Z. Yang and Q. Wang, *Journal of Alloys and Compounds*, 2016, **662**, 118–125.
- 34 J. Tan, M. Dun, L. Li, J. Zhao, W. Tan, Z. Lin and X. Huang, *Sensors and Actuators B: Chemical*, 2017, **249**, 44–52.